Journal of Chemical Neuroanatomy 40 (2010) 339–345

Contents lists available at ScienceDirect

Journal of Chemical Neuroanatomy

journal homepage: www.elsevier.com/locate/jchemneu

S1 to S2 hind- and forelimb projections in the agouti somatosensory cortex: Axon fragments morphological analysis

L.F. Santiago [a], E.G. Rocha [a], C.L.A. Santos [a], A. Pereira Jr[b], J.G. Franca [c], C.W. Picanço-Diniz [a,*]

[a] Universidade Federal do Pará, Laboratório de Investigações em Neurodegeneração e Infecção, Hospital Universitário João de Barros Barreto, Rua dos Mundurucus 4487, 66073-000 Belém, PA, Brazil
[b] Edmond and Lily Safra International Institute of Neurosciences of Natal (ELS-IINN), Rua Prof. Francisco Luciano de Oliveira 2460, 59066-060 Candelária, Natal, RN, Brazil
[c] Institute of Biophysics Carlos Chagas Filho, Federal University of Rio de Janeiro, Rio de Janeiro, RJ, Brazil

ARTICLE INFO

Article history:
Received 22 June 2010
Received in revised form 6 September 2010
Accepted 26 September 2010
Available online 27 October 2010

Keywords:
Somatosensory cortex
S1 to S2 projections
Axon morphology
Cluster analysis
Agouti
Dasyprocta prymnolopha

ABSTRACT

The integration of cutaneous, proprioceptive, and motor information in area S2 seems to be essential for manual object recognition and motor control. Part of the inputs to S2 comes from area S1. However no detailed investigations of the morphology of this projection are available. In the present study we describe and quantify the morphology of axon fragments of S1 to S2 ipsilateral projections in the agouti somatosensory cortex. Two groups of projecting axon arbors in S2 were individually reconstructed in three dimensions using Neurolucida, after a single electrophysiological guided BDA injection in either the forelimb ($n = 4$) or the hindlimb ($n = 4$). Electrophysiological mapping was performed 15 days after injections, allowing the localization of S2. Cluster analysis of 40 fragments after hindlimb and 40 after forelimb distinguished two clusters of terminals designated as type I and type II. On average, Type I fragments had greater surface areas and segment lengths than type II fragments, whereas type II fragments had higher number of terminal boutons, number of segments and branching points/mm than type I fragments. Type I corresponded to 58% of the axons projecting from the hindlimb representation in S1 whereas 63% of the sample originating from the forelimb representation in S1 corresponded to type II axons. The results suggest possible parallel processing by two stereotyped classes of axon terminals in the S1 to S2 projections that may represent at least part of the circuitry groundwork associated with distinct somatomotor skills of these limbs in agoutis.

1. Introduction

The majority of mammals share a common pattern of at least six somatosensory areas in the somatosensory cortex: the primary and secondary somatosensory cortical areas (S1 and S2), the parietoventral area (PV), the parieto-rhinal area (PR), and a somatosensory rostral (SR) and caudal (SC) fields adjoining S1 (Kaas and Collins, 2001; Henry et al., 2006). In contrast to other sensory systems, each of these somatosensory cortical fields is uniquely innervated by multiple thalamic nuclei (Padberg et al., 2009). Previous studies have reported that S2 receives topographic projections from ipsilateral S1 in monkeys (Jones et al., 1975, 1978; Friedman et al., 1986), cats (Jones and Powell, 1968; Manzoni et al., 1979; Burton and Kopf, 1984), tree shrews (Weller et al., 1987), and squirrels (Krubitzer et al., 1986). In rodents, S1 and S2 were first identified in mice, rats and grey squirrel (Woolsey and Van der Loos, 1970; Welker and Woolsey, 1974; Nelson et al., 1979; Carvell and Simons, 1987; Koralek et al., 1990; Fabri and Burton, 1991). Both areas receive projections from the same nuclei of the dorsal thalamus and are proposed to be nodes of equivalent hierarchy along parallel streams of the thalamocortical system that process light tactile stimuli (Kwegyir-Afful and Keller, 2004). More recently S1 and S2 forepaw representations in the rat brain were electrophysiologically recorded and iontophoretically injected with biotinylated dextran amine (BDA) and topographic, symmetric and reciprocal projections were demonstrated (Liao and Yen, 2008). In mice brain, similar organization was detected with prominent reciprocal projections between the barrel fields of S1 and S2 (Aronoff et al., 2010). However, no detailed morphometric analysis of S1 to S2 axonal projections to complement those assays are available.

Small lysencephalic rodents such as squirrel (Krubitzer et al., 1986), mice (Carvell and Simons, 1986, 1987) and rat (Koralek et al., 1990) were previously used to study somatosensory cortical projections but no studies are available in larger lisencephalic brains, where non primary areas are proportionally larger and detailed mapping procedures less difficult to perform. In the present report we focused our attention on the agouti, a diurnal

* Corresponding author. Tel.: +55 91 32016756; fax: +55 91 32016756.
E-mail address: cwpdiniz@gmail.com (C.W. Picanço-Diniz).

0891-0618/$ – see front matter © 2010 Elsevier B.V. All rights reserved.
doi:10.1016/j.jchemneu.2010.09.005

Hystricomorpha rodent with several species belonging to the single genus Dasyprocta. The agouti is native of tropical America and has a medium-sized body (about 3.5 kg) and a large lisencephalic brain. In agouti brain, previous architectural, electrophysiological, and hodological analyses confirmed the presence of S1 and S2 in the parietal cortex (Pimentel-Souza et al., 1980; Santiago et al., 2007). In addition we previously described based on cluster analysis and cortical multiunit electrophysiological recording after cutaneous stimulation, that callosal axon fragments of S1 hind- and forelimb representations in this species also revealed two types of morphologies of terminal axon fragments. Type I fragments were more frequent in hindlimb than in forelimb representation whereas most of type II axon arbors were found in the forelimb representation suggesting that the sets of callosal axons connecting fore and hindlimb regions in S1 are morphometrically distinct from each other (Rocha et al., 2007).

In the present study, we hypothesize that this dual morphological pattern of axon fragments might extend to the ipsilateral projections of hind- and forelimbs from area S1 to area S2. To investigate this hypothesis, computer-assisted reconstructions of axon fragments from different regions in S2 were assembled following a previously established protocol (Amorim and Picanco-Diniz, 1997; Gomes-Leal et al., 2002; Rocha et al., 2007). More specifically, we sampled BDA-labeled axon arbors in S2 after injection of the tracer in S1, either in the representation of the forepaw or the hindpaw wich were localized by multiunit electrophysiological recording. Based on cluster and discriminant analyses of the morphological features of axon fragments, we demonstrated in the present report the existence of two morphologically distinct channels distributed in different proportions in the hind and forelimbs projections from S1 to S2 ipsilateral cortical projections.

2. Materials and methods

2.1. Surgical procedures, electrophysiological recordings, and tracer injections

Eight adult agoutis (*Dasyprocta prymnolopha*) weighing 2.7–3.2 kg received a single injection of the anterograde tracer biotinylated amine (BDA, 10 kD, Molecular Probes, Eugene, OR) in area S1 of the left hemisphere. The injections were aimed either in the representation of the forelimb ($n = 4$) or of the hindlimb ($n = 4$), which were assessed by multiunit mapping before the injection. All experimental procedures followed the Principles of Laboratory Animal Care (NIH publication No. 86-23, revised 1985) and the local ethics committee on experimental animal research at the Federal University of Para, Brazil. The subjects used in the present investigation were donated by the Emilio Goeldi Zoo-Botanic Museum under the license of the Brazilian Institute of the Environment and Federal University of Para.

One day before the recording session, each animal was pre-medicated with 1.0 mg/kg intramuscular (i.m.) dexamethasone (Decadron, Prodome) to prevent brain edema and 1.0 mg/kg i.m. vitamin K (Kanakion, Roche) to minimize bleeding. The following day, anesthesia was induced by i.m. injection of a mixture of ketamine (10 mg/kg) and xylazine (1 mg/kg). The anesthetic level was monitored by testing the corneal reflex and supplementary doses were administered as needed. Body temperature was maintained at 37 °C. All efforts were made to use as few animals as possible and to minimize unnecessary animal discomfort, distress, and pain.

The head of the animal was secured with ear and mouth pieces in a standard head holder (David Kopf, Germany) and a craniotomy was performed to expose part of the left parietal cortex. Varnish-insulated tungsten microelectrodes (1 M at 1 kHz; FHC, Bowdoinham, ME) positioned with a micromanipulator were used to explore cortical multiunit activity (David Kopf). The multiunit signal was differentially amplified, bandpass-filtered between 1 and 3 kHz (ME04011, FHC), and fed simultaneously to a dual-beam storage oscilloscope (1476A, BK precision, Yorba Linda, CA) and audio monitor (SR771, Sansui, Japan). Somatosensory cortical mapping was performed with mechanical stimuli consisting of light touches with fine probes and brushes and displacement of hairs. After determining the injection site, a single pressure injection of 0.05 μL 10% BDA diluted in 0.1 M phosphate buffer (PB, pH 7.4) was made through a glass capillary of 40–50 μm of internal tip diameter. The animals were allowed to recover in the colony with ad libitum food and water. After a survival interval of 15–30 days, the animals were anesthetized again and submitted to a more detailed multiunit mapping of the left somatosensory areas, including S2. In order to localize the recording sites in the histological sections obtained afterwards, electrolytic lesions were produced by applying negative pulses of 10 μA for 10 s. A digital photograph of the exposed cortex was used to mark the recording and lesion sites. At the end of the experiment, the animals were deeply anesthetized and perfused through the aorta with warm 0.9% saline solution followed by 4% paraformaldehyde in 0.1 M PB.

2.2. Histological procedures and anatomical reconstructions

In all subjects the neocortex of both hemispheres was separated from subcortical structures and flattened between two glass slides overnight in fixative for flattening. The tissue was then cut on a vibratome (Pelco 1000, Ted Pella, Redding, CA) to obtain 100 μm-thick serial, tangential sections. Recording and injection sites were identified in the sections using the electrolytic lesions as landmarks. Serial tangential sections from the injected hemispheres were processed to reveal BDA-labeled ipsilateral axons. All sections were incubated overnight in avidin–biotin complex (ABC, Vector Laboratories, Burlingame, CA; 1:200) and processed for the nickel-enhanced DAB reaction protocol (Shu et al., 1988). Finally, sections were mounted on gelatinized slides, dehydrated, cleared, and coverslipped with Entellan (Merck, Darmstadt, Germany).

Two-dimensional reconstructions of the flattened hemispheres were achieved by superimposing drawings of individual tangential obtained by means of a camera lucida attached to a Stemi Zeiss stereoscope. Adjacent sections were aligned by matching anatomical landmarks and lesions. Thus, the injection site and the BDA-labeled axonal clusters identified in individual tangential sections were correlated with the electrophysiological map.

Three-dimensional (3D) reconstructions of individual axonal arbors were obtained by direct digitalization of the BDA-reacted sections, using a 60x oil immersion objective on an Optiphot-2 (Nikon, Japan) microscope equipped with a motorized stage (MAC200, LUDI, Hawthorne, NY) and coupled to a computer running the Neurolucida software (MicroBrightField, Colchester, VT). The x, y, and z coordinates of digitized points of the axon arbor was stored and then analyzed. For the purpose of the present investigation, an axon terminal was chosen for digitalization if it comprised an entire segment with most of its branches included in that same tangential section. We have chosen axon terminals that presented as many real true ends within a single section as possible. Smaller axonal arbors with thicker cut ends were not included in the sample.

A number of morphometric features were measured, including branching points, segments, and boutons per millimeter of axon length. Average densities were calculated by dividing the total number of appendages (branching points, segments, or boutons) by the total axon length, which was obtained by the sum of all intermediate segment lengths. The planar branching angle (in degrees) was measured between each pair of segments at all branching points in the plane defined by two rays drawn from the beginning of a branch to the next node or ending. The surface area of the axon terminal was calculated on the basis of the diameters assigned to different parts of the processes while tracing them. The start and end points of each line segment has a radius value determined by the size of the circular inset of the cross-hair cursor used when tracing. The surface area of each line segment is computed using these radius values and the length of each line segment in the formula for the surface area of a shape known as Right Frustrum. These calculations treat each process segment as a right frustum: (Lateral) surface area = pi × (R1 + R2) × sqrt ($(R1 - R2)^2 + L^2$), where R1 is the radius at the start of the line segment, R2 is the radius at the end of line segment and L is the length of line segment (Keller, 1908; MicroBrightField, 2000). Except by area measurements, all morphometric features were expressed in density values (number of occurrences of each feature per fragment, divided by total length of the fragment in millimeters). Thus, the result in each case was not affected by terminal size, incompleteness of labeling or visualization (Gomes-Leal et al., 2002; Rocha et al., 2007).

2.3. Statistical analysis

Statistical analyses followed similar procedures as those described elsewhere (Steele and Weller, 1995; Schweitzer and Renehan, 1997; Gomes-Leal et al., 2002). First, we submitted all quantitative morphometric variables of our sample to an initial cluster analysis including: branch density, segment density, boutons en passant density, terminal boutons density, segment length, terminal area, planar angle of bifurcations. The classes of axons suggested by the cluster analysis were further assessed by a forward stepwise discriminate function analysis using the software program Statistic 6.0 (Statsoft, Tulsa, OK) in order to determine which variables discriminate between two or more naturally occurring groups. This procedure determines whether groups differ with regard to the mean of a variable, and then uses that variable to predict group membership, revealing which variable provides the best separation of classes suggested by the cluster analysis. In addition, the arithmetic mean and standard deviation were calculated for the variables chosen as the best predictors for the groups. 10–16 Terminals from each subject were submitted to multiple measurements using dedicated software (Neuroexplorer, MicroBrightField) to process quantitative data obtained with Neurolucida.

On rare occasions, outliers were detected and excluded from all samples based on standard deviation using a standard statistical test to detect extreme values in the sample (Ayres et al., 2007). A parametric statistical analysis was carried out and a two-tailed Student's t-test for two related samples was used to compare axonal

Table 1
Summary of the experimental cases and labeling.

Subject	Injection site	Delivery procedure/ histochemical reaction	Sectioning plane
Da 06	FL (S1)	Pressure/BDA	Tangential
Cc 10	FL (S1)	Pressure/BDA	Tangential
PV 07	FL (S1)	Pressure/BDA	Tangential
Cc 12	FL (S1)	Pressure/BDA	Tangential
Cc 17	HL (S1)	Pressure/BDA	Tangential
Da 10	HL (S1)	Pressure/BDA	Tangential
Cc 11	HL (S1)	Pressure/BDA	Tangential
Cc 16	HL (S1)	Pressure/BDA	Tangential

BDA = biotinylated dextran amine, S1 = primary somatosensory area, FL = forelimb, HL = hindlimb.

groups suggested by the multivariate data analysis. Significance was accepted at 95% confidence level ($p < 0.05$).

2.4. Microphotographs and image processing

Photomicrography was performed with a digital camera (Coolpix 950) attached to a Nikon microscope (Mod Optiphot-2). The brightness and contrast of the pictures were adjusted with Adobe Photoshop (San Jose, CA) cs2 software.

3. Results

Table 1 summarizes the experimental cases analyzed in this study. Eighty projecting axon terminals in S2 were reconstructed, being 40 labeled after an injection in the forelimb representation in S1 and other 40 after a S1 hindlimb representation injection. The axon arbors were located mainly within layers II and III, as estimated by the superimposition of adjacent tangential sections. Nevertheless, some arbors also extended to layers V and VI. Axon arbors were digitized by the Neurolucida system and were further analyzed using the Neuroexplorer software.

3.1. Injection sites and pattern of ipsilateral labeling

Fig. 1 illustrates a single injection site in the forelimb representation in area S1. In the different cases, injection site diameter varied between 0.4 and 2.5 mm, and was characterized by a central black core circumscribed by a less dense halo containing cell bodies, dendrites, and well defined axon fragments.

Fig. 2 illustrates somatosensory maps, injection sites and location of ipsilateral intrinsic and extrinsic projections obtained after BDA injections in S1 forelimb (Fig. 2A) or hindlimb (Fig. 2B) representations. All cases revealed axon fragments oriented orthogonal and parallel to the pial surface. In all cases, ipsilateral and contralateral axonal clusters were identified both in homo- and heterotopic locations in S2 similar to what has been previously reported.

3.2. Morphology of S1 to S2 ipsilateral axon fragments

Fig. 3 illustrates typical axon fragments and 3D reconstructions found in S2 forelimb and hindlimb cortical representations. Notably, the hindlimb axon fragments presented less branching and fewer boutons than the forelimb arbors, whereas the thicknesses of both samples were similar.

3.3. Morphometry and multivariate statistical analysis of axon fragments from projections of S1 to S2 forelimb and hindlimb cortical representations

Fig. 4 illustrates the results of the cluster analysis of axonal fragments of S2 hindlimb and forelimb representations. The discriminant analysis is presented in Table 2. Two distinct clusters

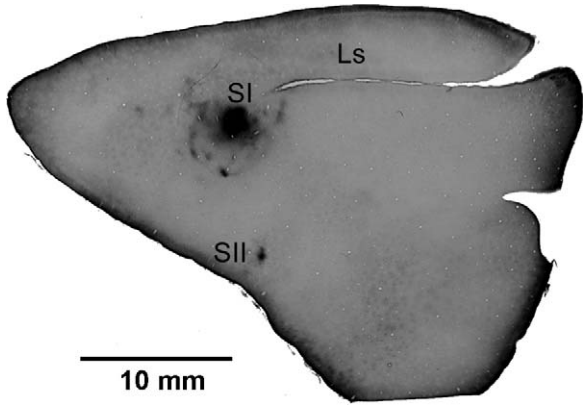

Fig. 1. Photomicrograph of the tracer injection of case Da 06 localized at the forelimb representation in agouti S1. Note a larger focus of labeling in the lateral cortex (S2) and smaller labeled spots around the injection site in S1. Ls = Lateral sulcus. Scale bar = 10 mm.

of fragments (type I and type II) were observed. Type II axons represented 63% of the total forelimb sample, and type I represented 58% of the total hindlimb sample. The discriminant analysis detected surface area, segment length, and terminal

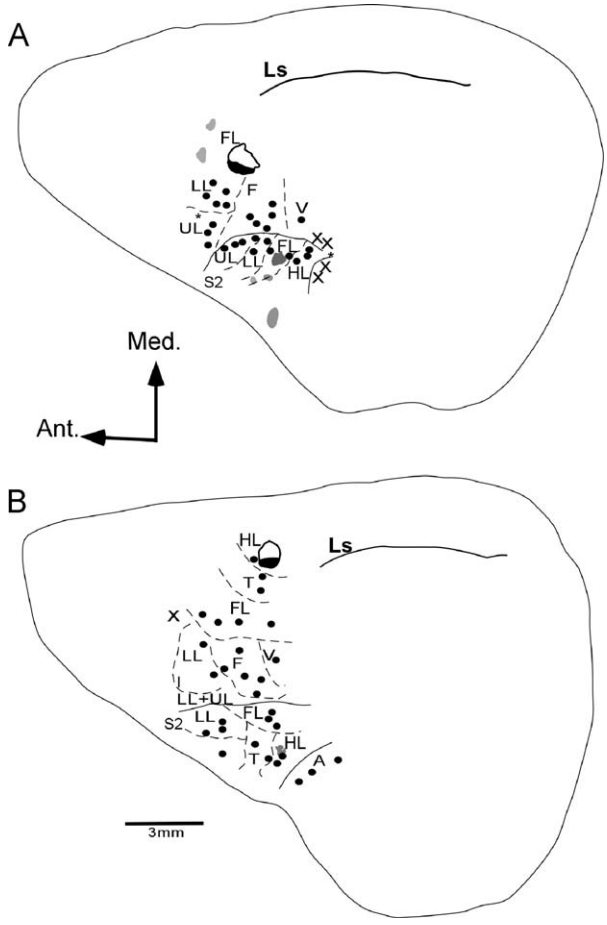

Fig. 2. Tangential reconstructions of hemisphere Da 07 (A), which received an injection in the forelimb representation of S1, and Cc 17 (B), which received an injection in the hindlimb representation of S1. Injection sites (black areas), recording sites (dots), BDA-labeled axon clusters (gray areas), and electrolytic lesions (asterisks) are represented. Thick lines represent the contours of the tangential section. Dashed lines define representational body areas on S1 and S2. Solid lines define the limit between S1 and S2. Ls = Lateral sulcus, FL = forelimb, HL = hindlimb, LL = lower lip, UL = upper lip, F = face, V = vibrissae, X = unresponsive, and A = auditory. Scale bar = 3 mm.

boutons density as the main variables for distinguishing between groups (Table 2). In addition, branching points and segment densities were significantly different between groups (two-tailed t-test, $p < 0.05$). Type I fragments had greater surface areas and segment lengths than type II fragments, whereas type II fragments had higher number of terminal boutons, number of segments and branching points/mm than type I fragments (Fig. 5, Table 3). Boutons en passant and branching angles were not significantly different (Table 3, $p > 0.05$). Except by these two features all other morphometric variables presented significant differences when comparing hindlimb and forelimb projections (Fig. 5; Table 3).

4. Discussion

We carried out at the first time a detailed comparison of the morphological characteristics of S1 to S2 ipsilateral projections to

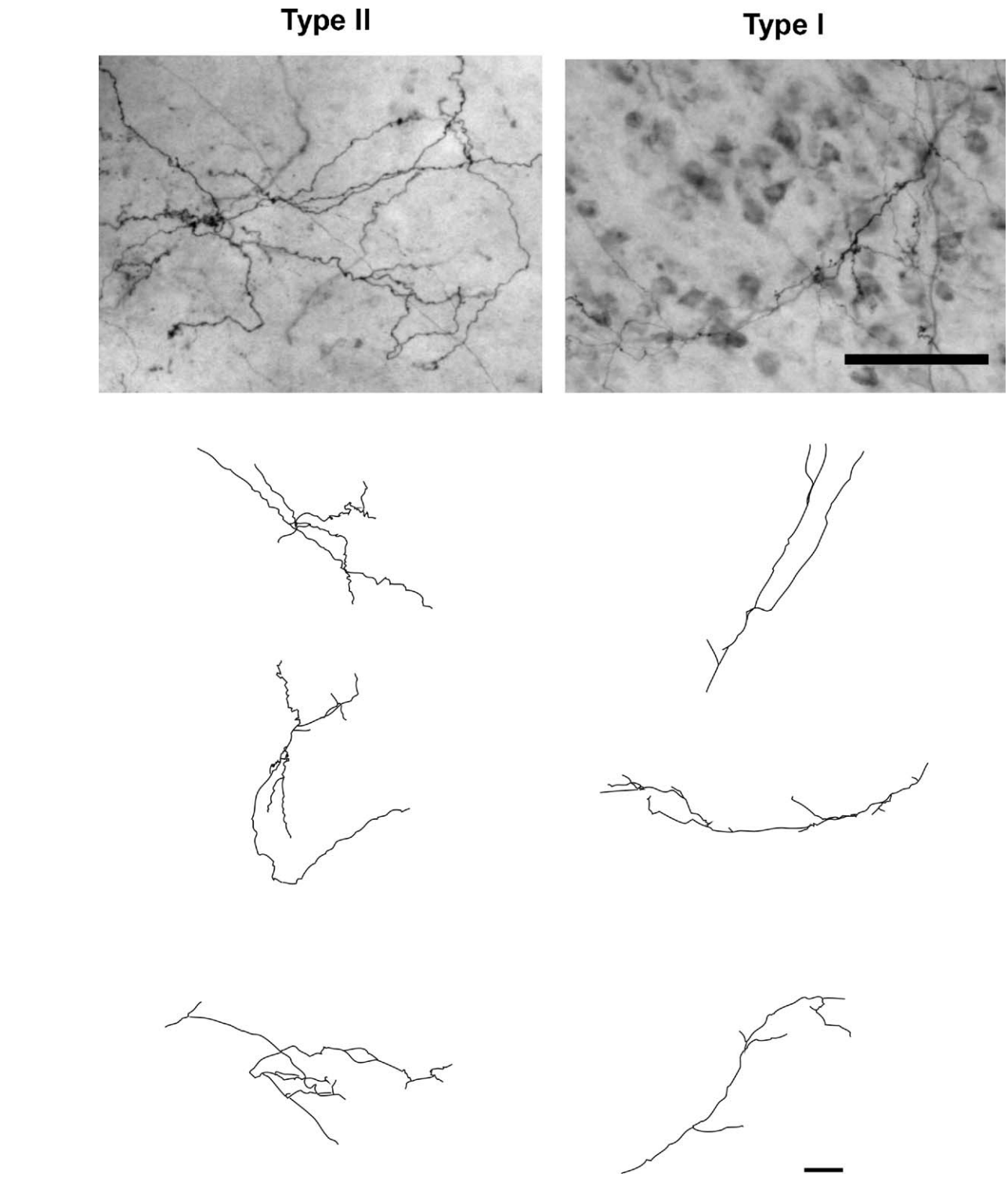

Fig. 3. Photomicrographs (top) and graphic representations (bottom) of the type II (A) and type I (B) axon fragments found in S2 after injection of BDA in agouti area S1. Axon terminal types were determined by cluster analysis, and the illustration selected fragments closer to the average values of the morphometric features of Types I and II with fine details of axonal morphology. Scale bars = 200 μm (top) and 50 μm (bottom).

compare morphometric properties of cortical axon fragments of hind- and forelimb representations in the agouti somatosensory cortex. Cluster and discriminant analysis of morphological parameters of 3D-reconstructed axon arbors detected two presumptive morphological groups that are distinguishable on the basis of surface area of axon terminal fields, segment length, and densities of number of segments and boutons terminaux. It was found that those two basic morphologies are distributed in different proportions in those topographical regions with a higher proportion of Type II in the forelimb as compared to the hindlimb representation.

4.1. Similar morphometric properties of axonal trees in different mammals

Previous studies in cat (Gomes-Leal et al., 2002) and *Cebus apella* striate cortices using iontophoretic biocytin injections demonstrated that intrinsic axons of those cortical regions can be distinguished in Types I and II on the basis of average segment length and density of axonal boutons, as revealed by cluster and discriminant analysis. In line with these descriptions, 3D reconstructions of entire axonal trees have revealed stereotypical morphological organization in the primary visual cortex of the adult cat (Martin and Whitteridge, 1984), suggesting that the branching pattern of axonal fragments may reproduce the branching properties of the whole axonal tree on a smaller scale. Topological analysis of these axon trees revealed that the axon branching pattern in the cat visual cortex is self-similar, with spiny and smooth neurons presenting similar levels of complexity (Binzegger et al., 2005). Interestingly, bouton densities inside an axonal cluster of an entire axon tree were reported to be four times higher for smooth neurons compared to spiny neurons (Binzegger et al., 2007).

S1 to S2 projections in agouti generally followed similar tendencies. The number of terminal boutons, branching points and segments per millimeter, were on average, 1.92, 1.64 and 1.84, times higher in type II than in type I axon fragments whereas terminal field area was 2.6 times smaller in Type II. In addition the comparison between morphometric features of axons from the hind- and forelimb representations revealed that boutons terminaux were on average, 4.5 times more frequent in the forelimb than in hindlimb fragments, whereas segment length was 57.6% shorter than hindlimb fragments. FL branching points and segments/mm were 4.15 and 1.50 times more frequent than hindlimb, with terminal fields 55% larger than HL axon arbors. Since forepaw representation was larger than hindpaw in S2 it is reasonable to expect larger arbors in S2 forepaw cortex. However still remain to be investigated why FL fragments present higher number of potential synapses and shorter segments than HL.

Table 2
Forward stepwise discriminant function analysis.

Variable	Wilks' lambda	Partial lambda	*F*-remove	*p*-Value	Tolerance
Area	0.836	0.457	89.992	0.000	0.971
Segment length	0.418	0.914	7.068	0.009	0.909
Terminal boutons	0.390	0.981	1.410	0.238	0.895

4.2. Possible implications of different morphologies in the hind- and forelimb S1 to S2 projections

Cluster and discriminant analysis of our axon fragments suggested two major groups of fragments projecting to S2 FL and HL representations: Types I and II. Type II axon terminals present more compact arborization, higher density of branching points and boutons terminaux/mm than Type I. The later presented longer and less ramified branches, running over longer cortical distances, but innervating a larger cortical area. Type II axons were more frequent in the forelimb and Type I in the hindlimb representations. Taken together, our data suggest that each fiber of S1 arriving in the S2 forelimb representation can recruit more neurons and potentially more synapses/mm than the hindlimb fibers for a same cortical volume. These two classes of agouti's axon fragments may represent morphological specializations related to different modalities of somatosensory information in order to homotopically interconnect S1 and S2 regions. Since bi-lateral sensorimotor behavior in the agouti is restricted to the forelimbs to manipulate food while eating and a higher proportion of Type II was found within the forelimb representation it may be worthwhile to investigate potential Type II axon contribution to this sensorimotor task. This observation is in line with our previous description of a similar profile of distribution in callosal connec-

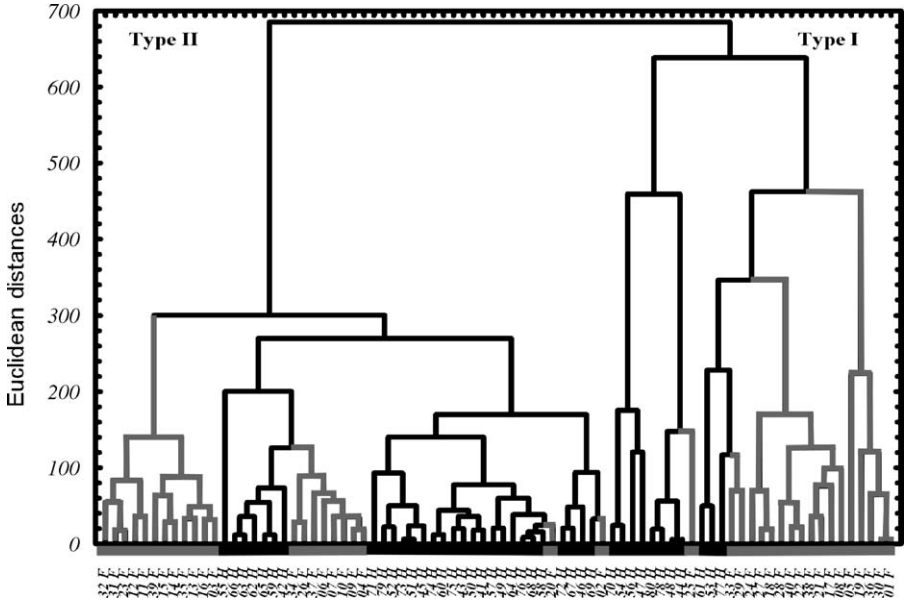

Fig. 4. Dendogram resulting from the cluster analysis. Eighty axon terminals were analyzed and their positions indicated in the clusters by Arabic numbers whose variables are depicted in Tables 2 and 3. The proposed classes of axons are designated as type I and type II. FL = forelimb (gray lines), HL = hindlimb (black lines).

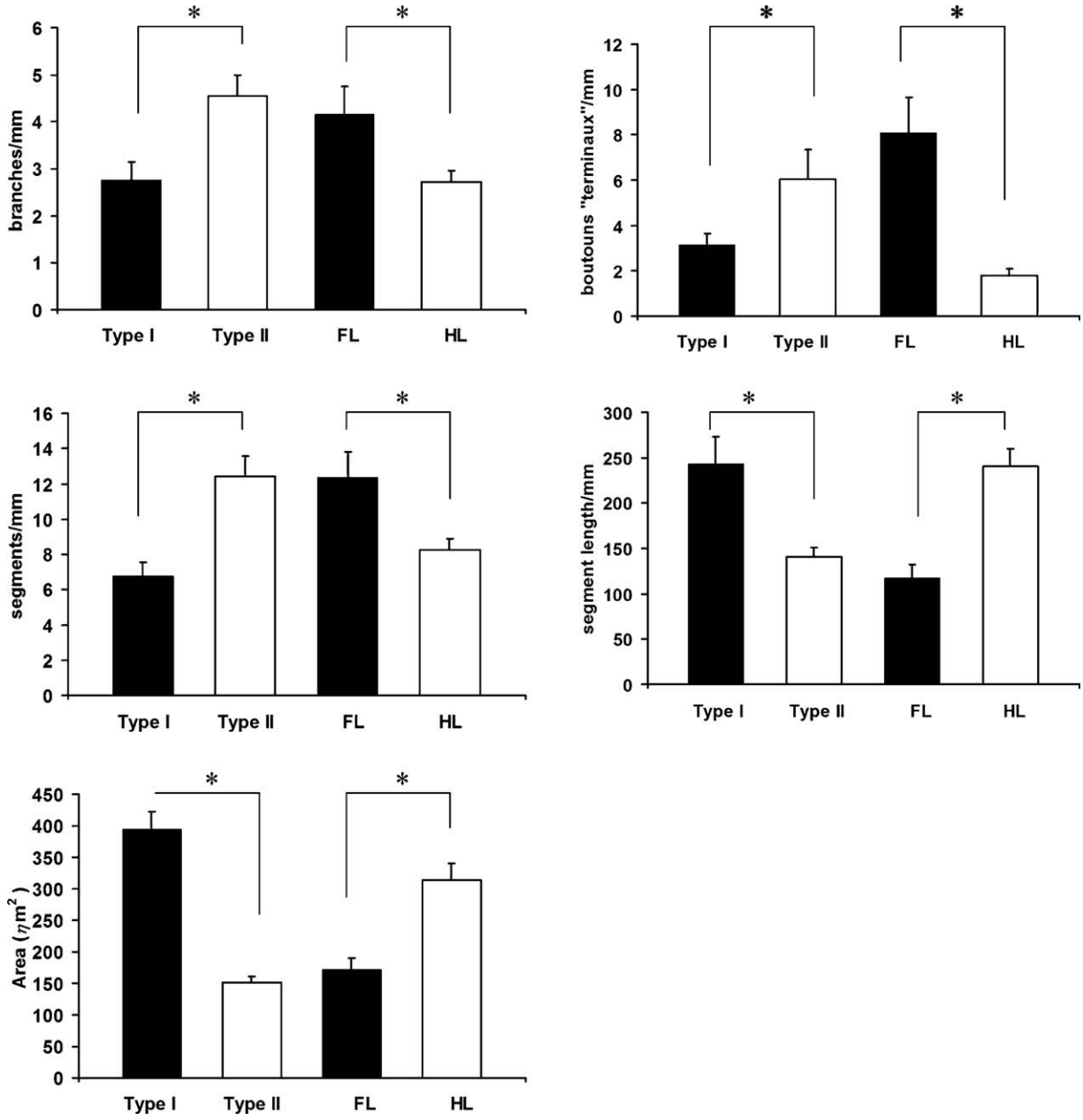

Fig. 5. Density of branching points (A), terminal boutons (B), and segments (C), segment length (D), and field area (E) of axon trees of the S1 to S2 somatosensory ipsilateral projections in the agouti. Significant distinctions between axon fragments Types I and II (left column) and between hind and forelimb (right column) are indicated by asterisk (two-tailed Student's *t*-test, $p < 0.05$). FL = forelimb, HL = hindlimb. Error bars represent standard error mean (s.e.m.).

tions where a higher proportion of Type II was also found in the forelimb as compared to hindlimb in S1 (Rocha et al., 2007).

4.3. Technical considerations

In three-dimensional anatomical reconstructions of axon terminals from single thick sections one has to assume that part of the axonal tree is located in adjacent sections. This implies in incomplete reconstructions from which only metric features that do not depend on the order of the segments are suitable for analysis. As previously recommended elsewhere (Amorim and Picanco-Diniz, 1997; Gomes-Leal et al., 2002; Rocha et al., 2007) we have done similar choice in the present morphometric analysis, providing consistent quantitative data through density values in

Table 3
Morphometric features of forelimb and hindlimb axon arbors.

Morphometric feature	I	II	*P*	FL	HL	*P*
Branching points/mm	2.77 ± 0.39	4.54 ± 0.45	0.0086	4.15 ± 0.60	2.73 ± 0.24	0.031
Boutons en passant/mm	19.07 ± 3.00	25.86 ± 3.09	0.1449	20.50 ± 2.44	22.98 ± 2.38	0.4704
Boutons terminaux/mm	3.13 ± 0.52	6.02 ± 1.33	0.0478	8.08 ± 1.56	1.80 ± 0.30	0.0003
Segments/mm	6.77 ± 0.78	12.44 ± 1.12	0.0005	12.38 ± 1.44	8.25 ± 0.64	0.0114
Segment length	243.57 ± 29.49	140.28 ± 10.84	0.0022	117.23 ± 15.32	240.80 ± 19.17	0.000
Terminal field area (μm)	394.80 ± 28.05	151.76 ± 9.00	0.000	172.33 ± 17.95	313.48 ± 26.43	0.000

selected axon terminals that presented as many real true ends within a single section as possible. Smaller axonal arbors with thicker cut ends were not included in the sample.

In agreement with previous research, our data revealed that the main differences detected by cluster and discriminant analyses between Types I and II terminals were due to the density of boutons and compactness of axonal trees with differential synaptic contributions.

Another technical limitation to be considered is related to the target areas of the reconstructed fragments. Indeed it has been described that S2 and parietal ventral (PV) areas adjoin along representations of forepaw and hindpaw in the rat brain (Remple et al., 2003). Assuming the occurrence of similar organization in agouti brain, it may be possible that not all reconstructed axon fragments were exclusively S2 axons since they possibly include both areas. However, because we did electrophysiological recordings to define S2 frontiers and as in the grey squirrel (Li et al., 1990) we have not detected PV area lateral to S2 in the agouti brain, it is reasonable to expect that all chosen fragments were taken from S2.

5. Conclusion

The results confirmed that S1 to S2 projections display different morphological domains, and suggest possible parallel processing by two stereotyped classes of axon terminals. The significant morphological differences observed in the fore- and hindlimb axon fragments may represent part of the circuitry groundwork associated with distinct somatomotor skills of these limbs in agoutis.

References

Amorim, A.K.J., Picanco-Diniz, C.W., 1997. Horizontal projections of area 17 in Cebus monkeys: metric features, and modular and laminar distribution. Braz. J. Med. Biol. Res. 30, 1489–1501.

Aronoff, R., Matyas, F., Mateo, C., Ciron, C., Schneider, B., Petersen, C.C., 2010. Long-range connectivity of mouse primary somatosensory barrel cortex. Eur. J. Neurosci. 31, 2221–2233.

Ayres M., Ayres Jr. M., Ayres D., Santos A.S., 2007. BioEstat 5.0: Aplicações estatísticas nas áreas das ciências biológicas e médicas. Belém: Sociedade Civil Mamirauá, Brasília CNPq.

Binzegger, T., Douglas, R.J., Martin, K.A., 2005. Axons in cat visual cortex are topologically self-similar. Cereb. Cortex 15, 152–165.

Binzegger, T., Douglas, R.J., Martin, K.A., 2007. Stereotypical bouton clustering of individual neurons in cat primary visual cortex. J. Neurosci. 27, 12242–12254.

Burton, H., Kopf, E.M., 1984. Ipsilateral cortical connections from the second and fourth somatic sensory areas in the cat. J. Comp. Neurol. 225, 527–553.

Carvell, G.E., Simons, D.J., 1986. Somatotopic organization of the second somatosensory area (SII) in the cerebral cortex of the mouse. Somatosens. Res. 3, 213–237.

Carvell, G.E., Simons, D.J., 1987. Thalamic and corticocortical connections of the second somatic sensory area of the mouse. J. Comp. Neurol. 265, 409–427.

Fabri, M., Burton, H., 1991. Ipsilateral cortical connections of primary somatic sensory cortex in rats. J. Comp. Neurol. 311, 405–424.

Friedman, D.P., Murray, E.A., O'Neill, J.B., Mishkin, M., 1986. Cortical connections of the somatosensory fields of the lateral sulcus of macaques: evidence for a corticolimbic pathway for touch. J. Comp. Neurol. 252, 323–347.

Gomes-Leal, W., Silva, G.J., Oliveira, R.B., Picanco-Diniz, C.W., 2002. Computer-assisted morphometric analysis of intrinsic axon terminals in the supragranular layers of cat striate cortex. Anat. Embryol. (Berl.) 205, 291–300.

Henry, E.C., Remple, M.S., O'Riain, M.J., Catania, K.C., 2006. Organization of somatosensory cortical areas in the naked mole-rat Heterocephalus glaber. J. Comp. Neurol. 495, 434–452.

Jones, E.G., Powell, T.P., 1968. The ipsilateral cortical connexions of the somatic sensory areas in the cat. Brain Res. 9, 71–94.

Jones, E.G., Burton, H., Porter, R., 1975. Commissural and cortico-cortical "columns" in the somatic sensory cortex of primates. Science 190, 572–574.

Jones, E.G., Coulter, J.D., Hendry SH, 1978. Intracortical connectivity of architectonic fields in the somatic sensory, motor and parietal cortex of monkeys. J. Comp. Neurol. 181, 291–347.

Kaas, J.H., Collins, C.E., 2001. The organization of sensory cortex. Curr. Opin. Neurobiol. 11, 498–504.

Keller, S.S., 1908. Mathematics for Engineering Students. Plane and Solid Geometry. D. Van Nostrand Company.

Koralek, K.A., Olavarria, J., Killackey, H.P., 1990. Areal and laminar organization of corticocortical projections in the rat somatosensory cortex. J. Comp. Neurol. 299, 133–150.

Krubitzer, L.A., Sesma, M.A., Kaas, J.H., 1986. Microelectrode maps, myeloarchitecture, and cortical connections of three somatotopically organized representations of the body surface in the parietal cortex of squirrels. J. Comp. Neurol. 250, 403–430.

Kwegyir-Afful, E.E., Keller, A., 2004. Response properties of whisker-related neurons in rat second somatosensory cortex. J. Neurophysiol. 92, 2083–2092.

Li, X.G., Florence, S.L., Kaas, J.H., 1990. Areal distributions of cortical neurons projecting to different levels of the caudal brain stem and spinal cord in rats. Somatosens. Motor Res. 7, 315–335.

Liao, C.C., Yen, C.T., 2008. Functional connectivity of the secondary somatosensory cortex of the rat. Anat. Rec. (Hoboken) 291, 960–973.

Manzoni, T., Caminiti, R., Spidalieri, G., Morelli E, 1979. Anatomical and functional aspects of the associative projections from somatic area SI to SII Experimental brain research. Experimentelle Hirnforschung 34, 453–470.

Martin, K.A., Whitteridge, D., 1984. Form, function and intracortical projections of spiny neurones in the striate visual cortex of the cat. J. Physiol. 353, 463–504.

MicroBright Field I (Eds.),2000. Neurolucida. MicroBrightField, Inc., Colchester, VT, www.microbrightfield.com.

Nelson, R.J., Sur, M., Kaas, J.H., 1979. The organization of the second somatosensory area (SmII) of the grey squirrel. J. Comp. Neurol. 184, 473–489.

Padberg, J., Cerkevich, C., Engle, J., Rajan, A.T., Recanzone, G., Kaas, J., Krubitzer, L., 2009. Thalamocortical connections of parietal somatosensory cortical fields in macaque monkeys are highly divergent and convergent. Cereb. Cortex 19, 2038–2064.

Pimentel-Souza, F., Cosenza, R.M., Campos, G.B., Johnson, J.I., 1980. Somatic sensory cortical regions of the agouti, Dasyprocta aguti. Brain Behav. Evol. 17, 218–240.

Remple, M.S., Henry, E.C., Catania, K.C., 2003. Organization of somatosensory cortex in the laboratory rat (Rattus norvegicus): evidence for two lateral areas joined at the representation of the teeth. J. Comp. Neurol. 467, 105–118.

Rocha, E.G., Santiago, L.F., Freire, M.A., Gomes-Leal, W., Dias, I.A., Lent, R., Houzel, J.C., Franca, J.G., Pereira Jr., A., Picanco-Diniz, C.W., 2007. Callosal axon arbors in the limb representations of the somatosensory cortex (SI) in the agouti Dasyprocta primnolopha. J. Comp. Neurol. 500, 255–266.

Santiago, L.F., Rocha, E.G., Freire, M.A., Dias, I.A., Lent, R., Houzel, J.C., Picanco-Diniz, C.W., Pereira Jr., A., Franca, J.G., 2007. The organizational variability of the rodent somatosensory cortex. Rev. Neurosci. 18, 283–294.

Schweitzer, L., Renehan, W.E., 1997. The use of cluster analysis for cell typing. Brain Res. Brain Res. Protoc. 1, 100–108.

Shu, S.Y., Ju, G., Fan LZ, 1988. The glucose oxidase-DAB-nickel method in peroxidase histochemistry of the nervous system. Neurosci. Lett. 85, 169–171.

Steele, G.E., Weller, R.E., 1995. Qualitative and quantitative features of axons projecting from caudal to rostral inferior temporal cortex of squirrel monkeys. Visual Neurosci. 12, 701–722.

Welker, C., Woolsey, T.A., 1974. Structure of layer IV in the somatosensory neocortex of the rat: description and comparison with the mouse. J. Comp. Neurol. 158, 437–453.

Weller, R.E., Sur, M., Kaas, J.H., 1987. Callosal and ipsilateral cortical connections of the body surface representations in SI and SII of tree shrews. Somatosens. Res. 5, 107–133.

Woolsey, T.A., Van der Loos, H., 1970. The structural organization of layer IV in the somatosensory region (SI) of mouse cerebral cortex, the description of a cortical field composed of discrete cytoarchitectonic units. Brain Res. 17, 205–242.